Mechanisms of Below-Threshold Harmonic Generation in Atoms

Wei-Hao Xiong,[1] Ji-Wei Geng,[1] Jing-Yi Tang,[1] Liang-You Peng,[1,2,*] and Qihuang Gong[1,2]
[1]State Key Laboratory for Mesoscopic Physics and Department of Physics, Peking University, Beijing 100871, China
[2]Collaborative Innovation Center of Quantum Matter, Beijing 100871, China
(Received 16 January 2014; published 9 June 2014)

Most previous studies have focused on high-order harmonic generation beyond the ionization threshold; mechanisms of below-threshold harmonics are less understood. We schematically study the harmonic emission process in this region by numerically solving the time-dependent Schrödinger equation of an atom in laser fields. We show that, besides the quantum path interference mechanism recently identified, the effects induced by the Coulomb potential also have a critical impact on these harmonics. These mechanisms can be distinguished in the structure of harmonic spectra by changing the laser wavelength and peak intensity. We find that the long quantum orbits can influence lower-order harmonics at a higher laser intensity. In addition, we show that the intensity-dependent steps of harmonic yield can disappear for certain harmonic orders, due to the trapping in the Rydberg states before recombination, which can explain recent experimental observations.

DOI: 10.1103/PhysRevLett.112.233001 PACS numbers: 32.80.Rm, 42.50.Hz, 42.65.Ky, 42.65.Re

The interaction of strong laser fields with atoms or molecules can lead to high-order harmonic generation (HHG), which can be applied as tabletop-coherent light sources in a wide frequency range [1–4]. The generation of these high-order harmonics can be understood by a semiclassical three-step model: the electron's tunneling ionization, its acceleration in the laser electric field, and its recombination with the ionic core [5,6]. In this scenario, strong-field approximation (SFA) can identify the trajectories of the particular electron that contribute to some specific harmonics and, thus, can give an intuitive understanding of the HHG process via the quantum path interference [7].

Most previous studies have concentrated on the harmonic generation beyond the ionization threshold. Less attention has been paid to the below-threshold harmonics (BTH), which were thought to be perturbative responses to the external laser field [8]. Several experiments were carried out for BTH in an elliptically polarized field [9–11] in the 1990s. An anomalous ellipticity dependence of harmonic yield was observed for a certain order of BTH. A theoretical study based on the Coulomb-corrected SFA was developed to partially explain the anomaly [12], but this method cannot explain the atomic species dependence observed in Ref. [11].

Very recently, Yost *et al.* [13] showed that high-repetition BTH can be applied to generate the frequency comb in the vacuum-ultraviolet range [14,15]. By exposing Xe into an intense 1070-nm driving laser field at different intensities, they observed interference in the harmonic yield of BTH, which indicates that there are contributions of long quantum orbits from electrons accelerated in the laser field for about one optical cycle. Soon after, negative dispersion was observed in BTH of a Keldysh-scaled system of Cs in a 3.6-μm laser [16], which also indicates nonperturbative quantum orbits have an effect in this range. Moreover, the different contributions from the generalized short and long quantum orbits were clearly identified in near-threshold harmonics from aligned molecules [17]. All of these experimental observations suggest new mechanisms for BTH beyond the perturbation theory.

Several theoretical studies for BTH have been carried out [18–20]. The conventional three-step model for HHG is not directly applicable to this region, though its generalization can be used to qualitatively understand the process [17,20]. In the generalized model, the Coulomb potential is taken into consideration during the acceleration process, and electrons ionized around the maximum of the laser electric field will contribute to BTH. When these electrons return to the core after about one optical cycle, they may acquire negative total energies; this can lead to the emission of a photon with energy less than the ionization potential I_p. The superposition of these long quantum orbits and short orbits with a near-zero phase has been used to explain the prominent intensity-dependent steps of these harmonics. However, both experiment and *ab initio* calculations in Ref. [13] observed less-pronounced steps for the ninth harmonic in Xe, which suggests that competing mechanisms, other than the quantum path interference, may exist. One natural question is whether abundant excited states have any effects on the generation of BTH.

In this Letter, we schematically investigate BTH by numerically solving the time-dependent Schrödinger equation (TDSE) with a real Coulomb potential of atomic hydrogen. Unlike the previous investigations of BTH, where only the laser intensity was scanned, we vary both the laser wavelength [21,22] and peak intensity to identify possible mechanisms of BTH. We find that, besides the

quantum path interference mechanism, resonance effects [23–25], both in the photon absorption and photon emission step, also have a crucial impact on the generation of BTH. The resonance mechanism reveals the influence of the Coulomb potential on the harmonic generation. We can identify different signatures of these two mechanisms in BTH.

The details of the numerical solution to the TDSE can be found in our previous work [26–28]. All spatial and temporal parameters are varied to make sure all the harmonic spectra are fully converged. In Fig. 1, we show yields of harmonics up to order 15 at a peak intensity of $I_0 = 6 \times 10^{12}$ W/cm^2, with various wavelengths from 702 to 1080 nm (a 20-cycle $\sin^2$ pulse is used for each wavelength λ). As seen from this Figure, the spectra from fifth to eleventh order vary drastically with the change of λ and show very complicated structures, which cannot be explained solely by the quantum path interference. Indeed, in the BTH region, the resonance effects with respect to the excited states can also dramatically change the harmonic yields. Besides the expected odd harmonics, emissions of almost-fixed photon energies at all wavelengths can also be observed in Fig. 1. The most prominent of such emissions is at the photon energy of 0.375 a.u., which corresponds to the bound-bound transition from $2p$ to $1s$ state. These emissions are similar to the atomic line emission, recently observed in experiments along with the harmonic generation [29–31]. When the bound state energy difference approximately matches multiples of the photon energy, the electrons can be pumped to $2p$ state through a multiphoton absorption. This mechanism will be discussed in the following paragraph as resonance absorption. For the wavelengths for which the photon energies do not satisfy the resonance condition, our studies show that the excitation mechanism can be a quasistatic excitation (for details, see Sec. A of the Supplemental Material [32]) since it is insensitive to the wavelength and the laser ellipticity. The ellipticity insensitiveness for this excitation mechanism may be related to the experimentally observed abnormal ellipticity dependence for a certain order of harmonic [9–11]. Because this kind of excitation is quite weak compared with multiphoton excitation, it will not influence the signal of odd harmonics we discuss in the following, where multiphoton absorption dominates.

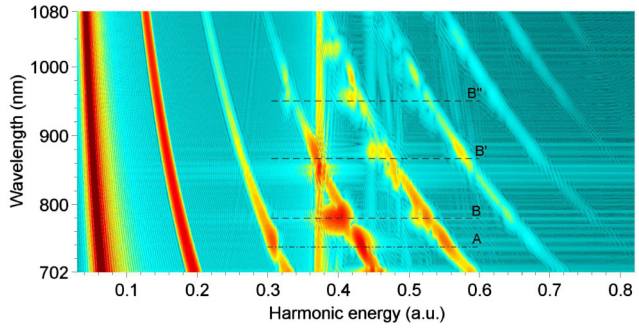

FIG. 1 (color online). Harmonic spectra of hydrogen interacting with an intense driving laser at a peak intensity $I_0 = 6 \times 10^{12}$ W/cm^2, with the laser wavelength changed from 702 to 1080 nm.

Hereafter, we will focus on the fifth, seventh, and ninth harmonics in Fig. 1. For better quantitative understanding of the BTH spectra, we integrate the harmonic yield within about one photon energy range for each harmonic. In Fig. 2, we show the integrated yield of the fifth, seventh, and ninth harmonics by changing the driving laser wavelength from 702 to 820 nm at different peak intensities. One can see that all three harmonics have a common feature, i.e., two series of peaks with different intensity dependence. Since the seventh harmonic has the clearest structures with two series of peaks [marked as A and B in Fig. 2(b)], we will first analyze this harmonic. Obviously, peak A barely changes with the intensity, while peak B shifts to a shorter wavelength as the peak intensity increases. These two peaks can be explained by the two different mechanisms mentioned above.

We first consider the multiphoton resonance absorption mechanism with respect to excited states. It should be noted that the multiphoton absorption (sensitive to the driving laser wavelength) is much stronger than the quasistatic excitation for the driving laser discussed here. When the energy difference between two ac Stark-shifted bound states matches $N\omega$, the yield of neighboring harmonic orders close to N can be significantly enhanced [23,24]. This enhancement is due to the higher probability of electron absorption photons when a bound state acts as

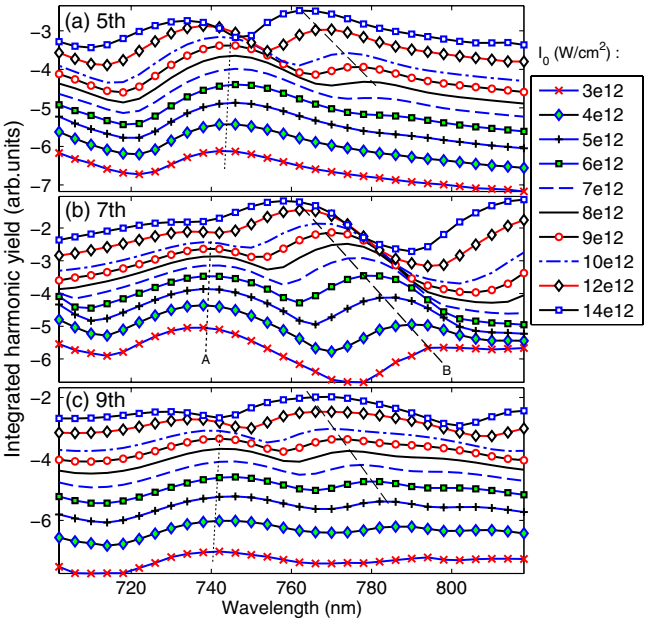

FIG. 2 (color online). The integrated harmonic yield for (a) fifth, (b) seventh, and (c) ninth harmonic as a function of the wavelength at various peak intensities.

an intermediate state. Thus, we denote this mechanism as "resonance absorption," to distinguish it from the "resonance emission" mechanism that will be discussed later. A multiphoton resonance absorption has features closely related to the properties of dressed bound states in a laser field. When the peak intensity increases, two main effects emerge: On the one hand, the wavelength of the resonance peak moves slightly because the energy difference between two bound states is quite stable against the change of I_0. On the other hand, the width of the resonance peak becomes broader due to the shorter lifetime of the excited states. In the present Letter, the positions of the resonance peaks are carefully identified for different intensities using the time-dependent autocorrelation method [33]. It turns out that most of the enhancement spots shown in Fig. 1 correspond to a multiphoton resonance absorption between low-lying excited states from $|n = 2\rangle$ to $|n = 5\rangle$ with respect to the ground state. Peak A shown in Fig. 2 is one of them, which can be identified as a six-photon resonance with the shifted $|n = 2\rangle$ state. When I_0 becomes even higher, the spectrum becomes so broad that there is practically no clear peak. In addition, peak B moves towards this wavelength range and further obscures the resonance peak A.

There are peaks in Fig. 1 that cannot be explained by resonance with any state. Peak B marked in Fig. 2(b) is one of them; it has a rather different behavior compared with peak A. In the following, we will show that peak B is related to the quantum path interference in BTH as recently discussed [17,20]. In the SFA picture, the quantum path interference is related to the channel closing number defined by $R = (U_p + I_p)/\omega$ [34], where $U_p = I_0^2/4\omega^2$ is the ponderomotive energy, I_p is the ionization energy, and ω is the driving laser frequency. Gentle peaks will emerge when R is a little smaller than an integer. The harmonic yields in BTH cannot be accurately estimated by the conventional SFA, while the concept of quantum orbits in SFA can be generalized to understand the phenomenon. For the case of BTH, the electrons with long quantum orbits will return to the core after its excursion in the laser field for about one optical cycle. From a simplified quantum path interference model [35], the superposition of these long orbits and the short orbits with a near-zero phase can lead to interference peaks spaced by $\delta R \approx 1$. These peaks are similar to the gentle peaks in SFA caused by the superposition of several trajectories. In Fig. 2, peak B at all laser intensities satisfies $R \approx 8.8$. In Fig. 1, there are at least two other noticeable peaks relating to the quantum path interference, which correspond, respectively, to $R \approx 9.8$ (at about 867 nm, which is not obvious due to several resonances nearby, marked as B' in Fig. 1) and $R \approx 10.8$ (at about 950 nm, marked as B'' in Fig. 1). These observations suggest that these peaks are mainly contributed to by the interferences of generalized short-long quantum orbits in the BTH region. We will come back to this point later for further confirmation.

Now let us turn to the integrated yield of the fifth harmonic shown in Fig. 2(a). Compared to the seventh harmonic, the fifth harmonic has roughly similar patterns in the resonance peak. However, one major difference for the fifth order is that peak B, related to the quantum path interference, is absent at peak intensities lower than 6×10^{12} W/cm^2, but gradually emerges as I_0 is further increased. To understand this phenomenon, we assume that for a lower laser intensity, the electrons with long quantum orbit have a larger return energy. When the return energy is not low enough to emit a photon corresponding to the fifth harmonic, one cannot observe the quantum path interference contribution in the harmonic spectra. Our assumption can be confirmed by the semiclassical model introduced in Ref. [20]. Here we use this model with a soft-core Coulomb potential to qualitatively analyze the above phenomenon. In Fig. 3(a), we show the semiclassical results for the lowest return energy of electrons by changing the laser peak intensity. As we can see, when the laser intensity increases, the lowest return energy drops. The lowest return energy is related to the lowest harmonic order to which the long quantum orbit can contribute. This confirms our assumption and explains why quantum path interference at the fifth harmonic emerges at higher laser intensities. To make this point more clear, we choose the electron with the lowest return energy and show in Fig. 3(b) its energy evolution with time after its ionization for three different peak intensities. We can see that for a higher intensity, the electron travels a longer time and returns to the core with a lower energy. This semiclassical investigation further

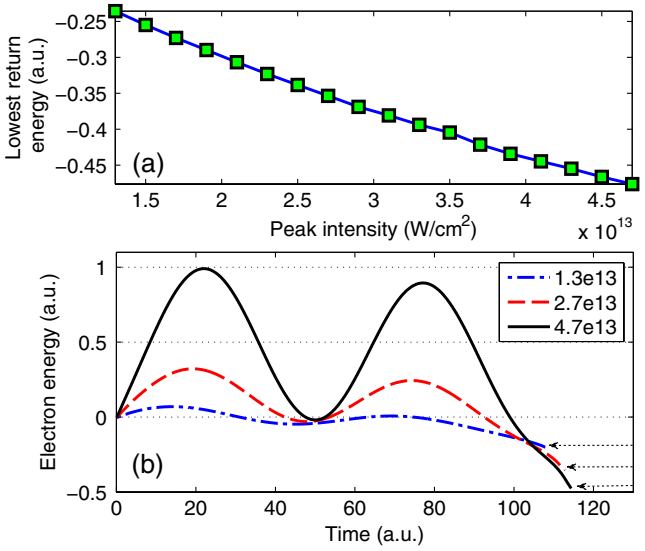

FIG. 3 (color online). (a) The lowest return energy as a function of the laser intensity calculated from the semiclassical model. (b) The evolution of the electron energy with time after ionization at three different laser intensities (W/cm^2). Each arrow indicates the moment and the energy when this electron recombines with the core.

confirms that peak B in the seventh harmonic [see Fig. 2(b)] indeed comes from the contribution of long quantum orbits.

Finally, we will look at the difference between the seventh and ninth harmonics, as shown in Figs. 2(b) and 2(c), respectively. Generally speaking, the ninth harmonic has structures qualitatively similar to those of the seventh, except that the quantum path interference peak B in the ninth order is much broader than that in the seventh order. This is caused by the other resonance mechanism: resonance in the recombination step. We call this mechanism the resonance emission. To understand this mechanism, we introduce a four-step model similar to that in Ref. [36]. In that model, the role of the autoionizing state was investigated, while here we pay attention to all of the excited states. The model can be described as follows: (1) ionization, (2) propagation in different trajectories, (3) trapping in the excited states when returning back to the core, and (4) emission of a photon. The existence of the being-trapped step can be verified through the harmonic spectra shown in Sec. B of the Supplemental Material [32]. The emitted photon energy shifted from the odd harmonics down to the atomic emission energy when the harmonic energy is slightly higher than the bound state energy. In the three-step model, trajectories with different phases in the propagation step cause the quantum path interference. For the four-step model, another phase will be induced in the trapping step. The additional phase is related to how long the electron stays in the excited state. For the ninth harmonic, many bound states can get involved at this wavelength range, which can cause broadening of the quantum path interference peak.

To illustrate this point, we investigate the intensity dependence of both the seventh and ninth harmonics at 810 and 790 nm, as shown in Figs. 4(a) and 4(b), respectively. For the 810 nm case, the ninth harmonic energy is resonant with high-lying Rydberg states, while the seventh harmonic is resonant with $2p$ state. The electrons that generate the ninth harmonic will be trapped in the high-lying Rydberg states, while those that generate the seventh harmonic can be captured by the $2p$ state. For the high-lying Rydberg states, a stable classical orbit can form, as been confirmed in the atom stabilization study [37]. In this kind of orbit, electrons can stay for a long time and can accumulate a phase comparable to the phase induced in the propagation step. However, the $2p$ state is not stable in a strong laser field [23], and the recombination happens immediately with a small phase accumulated (which can be ignored). Thus, for different excited states, different phases will be accumulated. When the phase is large enough, the interference structure can be smoothed or can even disappear. The expected results can be seen in Fig. 4(a); the yield of the ninth harmonic increases with the laser intensity rather smoothly, while the yield of the seventh shows prominent intensity-dependent steps. When the wavelength is tuned to 790 nm in Fig. 4(b),

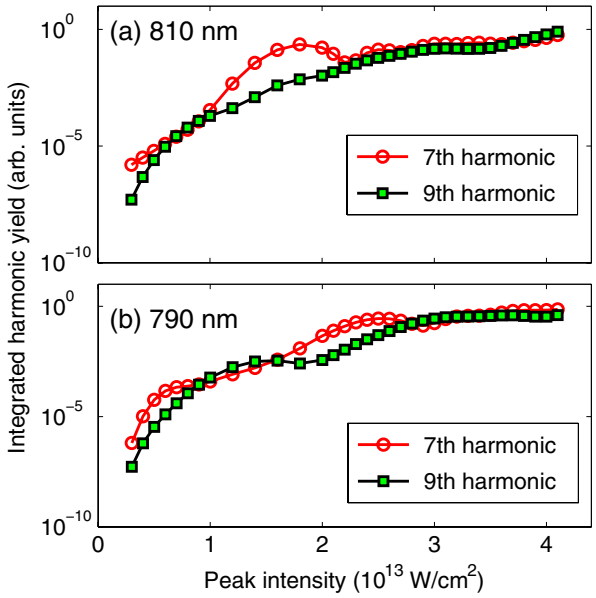

FIG. 4 (color online). Intensity dependence of the integrated harmonic yield for the seventh and ninth harmonic at two different laser wavelengths: (a) 810 nm and (b) 790 nm.

in which case no resonances with the high-lying Rydberg states can be prescribed, one can observe intensity-dependent steps in the harmonic yields of both the seventh and ninth harmonics. Similar structures at 645 nm, as well as a detailed verification, are shown in Sec. B of the Supplemental Material [32].

The intensity-dependent structures recently observed experimentally in Xe [13] are similar to the results of 810 nm here. After analyzing the energy levels of the Xe atom (shown in Sec. C of the Supplemental Material [32]), we think the smoothed ninth harmonic yield is also related to the influence of high-lying Rydberg states.

In conclusion, we have schematically investigated the BTH of atomic hydrogen with the Coulomb potential fully taken into consideration. A quasistatic excitation mechanism with weak signals is proposed, corresponding to atomic line emission for an off-resonance driving laser. For the odd harmonics usually investigated, two main mechanisms, including resonance mechanism and quantum path interference, are investigated. The signatures of two mechanisms have been identified by varying both the laser wavelength and peak intensity. For the quantum path interference mechanism, we find that for higher laser intensities, the long orbits can influence lower order harmonics. In the resonance mechanism, the BTH generation can be enhanced through resonance absorption. The structure of quantum path interference can be destroyed by the resonance emission if resonance happens with long-lifetime Rydberg states. In general, both mechanisms should be considered in order to understand the generation of BTH. We believe the present study reveals the complicated influence of the Coulomb potential in the harmonic

generation, which will be instructive for future experimental studies. Our study also demonstrates the important roles played by the Coulomb potential in strong-field processes, especially in the low-energy regime.

This work is supported by the 973 Program under Grant No. 2013CB922402, by the National Natural Science Foundation of China under Grants No. 11322437, No. 11174016, and No. 11121091, and by the Program for New Century Excellent Talents in University (NCET). The computational results were obtained by using the computer cluster "MESO" in the State Key Laboratory for Mesoscopic Physics at Peking University.

*liangyou.peng@pku.edu.cn

[1] T. Popmintchev *et al.*, Science **336**, 1287 (2012).
[2] M. Hentschel, R. Kienberger, Ch. Spielmann, G. A. Reider, N. Milosevic, T. Brabec, P. Corkum, U. Heinzmann, M. Drescher, and F. Krausz, Nature (London) **414**, 509 (2001).
[3] P. M. Paul *et al.*, Science **292**, 1689 (2001).
[4] F. Krausz and M. Ivanov, Rev. Mod. Phys. **81**, 163 (2009).
[5] P. B. Corkum, Phys. Rev. Lett. **71**, 1994 (1993).
[6] K. J. Schafer, B. Yang, L. F. DiMauro, and K. C. Kulander, Phys. Rev. Lett. **70**, 1599 (1993).
[7] M. Lewenstein, Ph. Balcou, M. Y. Ivanov, A. L'Huillier, and P. B. Corkum, Phys. Rev. A **49**, 2117 (1994).
[8] A. L'Huillier, K. J. Schafer, and K. C. Kulander, J. Phys. B **24**, 3315 (1991).
[9] N. H. Burnett, C. Kan, and P. B. Corkum, Phys. Rev. A **51**, R3418 (1995).
[10] K. Miyazaki and H. Takada, Phys. Rev. A **52**, 3007 (1995).
[11] M. Kakehata, H. Takada, H. Yumoto, and K. Miyazaki, Phys. Rev. A **55**, R861 (1997).
[12] M. Y. Ivanov, T. Brabec, and N. Burnett, Phys. Rev. A **54**, 742 (1996).
[13] D. C. Yost, T. R. Schibli, J. Ye, J. L. Tate, J. Hostetter, M. B. Gaarde, and K. J. Schafer, Nat. Phys. **5**, 815 (2009).
[14] C. Gohle, T. Udem, M. Herrmann, J. Rauschenberger, R. Holzwarth, H. A. Schuessler, F. Krausz, and T. W. Hänsch, Nature (London) **436**, 234 (2005).
[15] A. Cingöz, D. C. Yost, T. K. Allison, A. Ruehl, M. E. Fermann, I. Hartl, and J. Ye, Nature (London) **482**, 68 (2012).
[16] E. P. Power, A. M. March, F. Catoire, E. Sistrunk, K. Krushelnick, P. Agostini, and L. F. DiMauro, Nat. Photonics **4**, 352 (2010).
[17] H. Soifer, P. Botheron, D. Shafir, A. Diner, O. Raz, B. D. Bruner, Y. Mairesse, B. Pons, and N. Dudovich, Phys. Rev. Lett. **105**, 143904 (2010).
[18] J. C. Liu, M. C. Kohler, C. H. Keitel, and K. Z. Hatsagortsyan, Phys. Rev. A **84**, 063817 (2011).
[19] J. Henkel, T. Witting, D. Fabris, M. Lein, P. L. Knight, J. W. G. Tisch, and J. P. Marangos, Phys. Rev. A **87**, 043818 (2013).
[20] J. A. Hostetter, J. L. Tate, K. J. Schafer, and M. B. Gaarde, Phys. Rev. A **82**, 023401 (2010).
[21] K. Schiessl, K. L. Ishikawa, E. Persson, and J.Burgdörfer, Phys. Rev. Lett. **99**, 253903 (2007).
[22] K. L. Ishikawa, K. Schiessl, E. Persson, and J.Burgdörfer, Phys. Rev. A **79**, 033411 (2009).
[23] M. B. Gaarde and K. J. Schafer, Phys. Rev. A **64**, 013820 (2001).
[24] R. Taïeb, V. Véniard, J. Wassaf, and A. Maquet, Phys. Rev. A **68**, 033403 (2003).
[25] C. Figueira de Morisson Faria, R. Kopold, W. Becker, and J. M. Rost, Phys. Rev. A **65**, 023404 (2002).
[26] L.-Y. Peng and A. F. Starace, J. Chem. Phys. **125**, 154311 (2006).
[27] L.-Y. Peng, E. A. Pronin, and A. F. Starace, New J. Phys. **10**, 025030 (2008).
[28] M.-H. Xu, L.-Y. Peng, Z. Zhang, Q. Gong, X.-M. Tong, E. A. Pronin, and A. F. Starace, Phys. Rev. Lett. **107**, 183001 (2011).
[29] M. Sivis, M. Duwe, B. Abel, and C. Ropers, Nat. Phys. **9**, 304 (2013).
[30] A. Blättermann, C.-T. Chiang, and W. Widdra, Phys. Rev. A **89**, 043404 (2014).
[31] M. Chini, X. Wang, Y. Cheng, H. Wang, Y. Wu, E. Cunningham, P.-C. Li, J. Heslar, D. A. Telnov, S.-I Chu, and Z. Chang, Nat. Photonics **8**, 437 (2014).
[32] See Supplemental Material at http://link.aps.org/supplemental/10.1103/PhysRevLett.112.233001 for details about the quasistatic excitation, the resonance mechanism, and the energy levels of Xe atom.
[33] L.-Y. Peng, J. F. McCann, D. Dundas, K. T. Taylor, and I. D. Williams, J. Chem. Phys. **120**, 10046 (2004).
[34] D. B. Milošević and W. Becker, Phys. Rev. A **66**, 063417 (2002).
[35] A. Zaïr, M. Holler, A. Guandalini, F. Schapper, J. Biegert, L. Gallmann, U. Kellerl, A. S. Wyatt, A. Monmayrant, I. A. Walmsley, E. Cormier, T. Auguste, J. P. Caumes, and P. Salières, Phys. Rev. Lett. **100**, 143902 (2008).
[36] V. Strelkov, Phys. Rev. Lett. **104**, 123901 (2010).
[37] H. Liu, Y. Liu, L. Fu, G. Xin, D. Ye, J. Liu, X. T. He, Y. Yang, X. Liu, Y. Deng, C. Wu, and Q. Gong, Phys. Rev. Lett. **109**, 093001 (2012).